

Unconventional spin excitations in the $S = \frac{3}{2}$ triangular antiferromagnet $\text{RbAg}_2\text{Cr}[\text{VO}_4]_2$

S. Lee,^{1,2} R. Klauer,³ J. Menten,³ W. Lee,¹ S. Yoon,¹ H. Luetkens,⁴ P. Lemmens,^{5,6} A. Möller,^{3,*} and K.-Y. Choi^{1,†}

¹*Department of Physics, Chung-Ang University, 84 Heukseok-ro, 06974 Seoul, Republic of Korea*

²*ISIS Neutron and Muon Source, STFC Rutherford Appleton Laboratory, Harwell Campus, Didcot, Oxfordshire OX11 0QX, United Kingdom*

³*Department of Chemistry, JGU Mainz, Duesbergweg 10-14, 55128 Mainz, Germany*

⁴*Laboratory for Muon Spin Spectroscopy, Paul Scherrer Institute, 5232 Villigen PSI, Switzerland*

⁵*Institute for Physics of Condensed Matter, TU Braunschweig, Mendelssohnstrasse 3, 38106 Braunschweig, Germany*

⁶*Laboratory for Emerging Nanometrology, TU Braunschweig, Langer Kamp 6a/b, 38106 Braunschweig, Germany*



(Received 30 May 2019; revised manuscript received 13 April 2020; accepted 28 May 2020; published 12 June 2020)

We present muon spin relaxation (μSR) measurements of the $S = 3/2$ undistorted triangular lattice established in $\text{RbAg}_2\text{Cr}[\text{VO}_4]_2$. The zero- (ZF) and longitudinal-field μSR spectra evidence the absence of spin freezing and long-range magnetic ordering down to $T = 25$ mK, supporting the formation of a dynamic ground state. Noticeably, we observe an anomalous temperature dependence of the ZF muon spin relaxation rate $\lambda_{\text{ZF}}(T)$, featuring a decrease below $T = 20$ K. This suggests the alteration of the dominant relaxation mechanism by the development of short-range magnetic correlations. A subsequent leveling off of $\lambda_{\text{ZF}}(T)$ below $T = 2$ K indicates persistent spin dynamics and reveals the presence of exotic magnetic excitations. The field dependence of the muon spin relaxation rate at $T = 25$ mK is well described by a diffusive spin transport model with algebraic spin-spin correlations. The suppressed long-range order and the peculiar temperature-dependent behavior of $\lambda_{\text{ZF}}(T)$ will be discussed in terms of the exchange interaction between Cr^{3+} moments via nonmagnetic $[\text{VO}_4]^{3-}$ entities. In the title compound, the degeneracy of the t_{2g} -orbital set is not lifted by a space group symmetry reduction or subject to significant anisotropy resulting from spin-orbit coupling.

DOI: [10.1103/PhysRevB.101.224420](https://doi.org/10.1103/PhysRevB.101.224420)

I. INTRODUCTION

Following Wannier's pioneering work [1] on the triangular lattice (TL), this spin coordination has provided a fertile playground for novel states of matter. More significantly, it inspired the work on quantum spin liquids (QSLs) [2]. It is theoretically well established that antiferromagnetic Heisenberg spin systems on the undistorted triangular lattice exhibit a chiral 120° long-range magnetic order regardless of the spin magnitude [3–6]. The TL compounds $\text{A}\text{Ag}_2\text{Fe}[\text{VO}_4]_2$ ($A = \text{K}$ or Rb) [7] and $\text{RbFe}[\text{MoO}_4]_2$ [8] with $S = 5/2$ show this ground state, as predicted. In contrast, κ -(BEDT-TTF) $_2\text{Cu}_2(\text{CN})_3$, $\text{EtMe}_3\text{Sb}[\text{Pd}(\text{dmit})_2]_2$, and YbMgGaO_4 with $S = 1/2$ have been classified as QSL materials [9–11]. The suppression of long-range ordering (LRO) in TL has been discussed within different scenarios based on a proximity to a Mott transition or in the framework of a modified exchange Hamiltonian [1,12–16]. Therefore, the search for new QSL candidate materials is of fundamental interest in the context of tunable alterations induced through chemical composition.

Recently, a series of TL compounds $\text{A}\text{Ag}_2\text{Cr}[\text{VO}_4]_2$ ($A = \text{Ag}^+$, K^+ , and Rb^+) were reported. For $A = \text{Ag}^+$ collinear long-range magnetic order ($T_N = 10$ K) is observed. In

contrast, the absence of LRO down to 30 mK is reported for $A = \text{Rb}^+$ [17]. The latter intriguing observation places $\text{RbAg}_2\text{Cr}[\text{VO}_4]_2$ as a candidate for a QSL ground state. In $\text{A}\text{Ag}_2\text{Cr}[\text{VO}_4]_2$, Cr^{3+} ions ($S = 3/2$) constitute a triangular layer and interact with each other via nonmagnetic $[\text{VO}_4]^{3-}$ rigid units. The orientation of the $[\text{VO}_4]^{3-}$ entities varies with the size of the A site ion, which is found to tune the symmetry of the CrO_6 polyhedra and distort the TL.

For the smallest A cation (Ag^+) collinear LRO around $T_N \approx 10$ K is established. It is noteworthy that the symmetry (space group $C2/c$) also dictates the localization of the ordered magnetic moment in a single rectangular plaquette [see Fig. 1(a)]. The orientation of these moments within this plaquette was derived from neutron diffraction experiments [17]. The plaquette's corners mark the oxygen positions of the Cr coordination. The orbitally degenerate set (t_{2g}) in an octahedral ligand field of Cr^{3+} is represented by three orbitals. These orbitals intersect the edges of the depicted plaquettes.

The larger A site cations retain the threefold symmetry (space group $P\bar{3}$) of an undistorted TL [see Fig. 1(b)], and the degeneracy of the threefold orbital set is preserved [Fig. 1(c)]. It follows that for each Cr site the three plaquette orientations are geometrically equivalent. As an example, one of the manifolds of the distinct geometrically degenerate scenarios is illustrated in Fig. 1(c). This implies a highly degenerate ground state based on the superpositions of exchange pathways via $d_{\text{Cr}}\text{-}p_{\text{O}}\text{-}d_{\text{V}}\text{-}p_{\text{O}}\text{-}d_{\text{Cr}}$ on the undistorted TL.

*angela.moeller@uni-mainz.de

†kchoi@cau.ac.kr

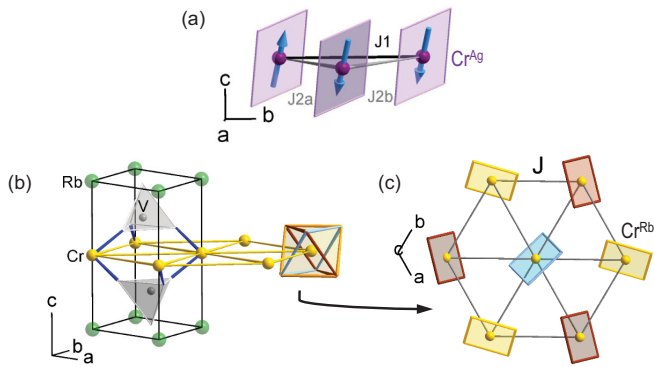


FIG. 1. (a) Orientation of the ordered magnetic moment within a uniquely defined rectangular plaquette at the Cr site (denoted Cr^{Ag}) for the distorted TL ($\text{AgAg}_2\text{Cr}[\text{VO}_4]_2$). (b) Crystal structure of the undistorted TL of $\text{RbAg}_2\text{Cr}[\text{VO}_4]_2$. For clarity, Ag and O atoms are not shown. The exchange paths between the Cr^{3+} ($S = 3/2$) ions are mediated by the nonmagnetic $[\text{VO}_4]^{3-}$ entities. Cr-O bonds are represented by blue sticks. The threefold degenerate orientation of the t_{2g} -orbital set is represented by the plaquettes (orange, red, and blue) per Cr site (Cr^{Rb}). (c) One of the possible electronic configurations is symbolized by the colored plaquettes.

Neutron diffraction and ac magnetic susceptibility show neither short- nor long-range magnetic order of the undistorted antiferromagnetic TL compound ($A = \text{Rb}$) down to 30 mK. The magnetic specific heat of $\text{RbAg}_2\text{Cr}[\text{VO}_4]_2$ indicates the preservation of 80% of the total magnetic entropy below $T = 2$ K in zero field despite a Curie-Weiss constant of $\Theta_{\text{CW}} = -10$ K. This implies the presence of an abundant low-energy density of states. As such, it is imperative to clarify whether the undistorted TL in $\text{RbAg}_2\text{Cr}[\text{VO}_4]_2$ eventually hosts a QSL ground state and to elucidate its origin and character by muon spin relaxation studies (μSR).

II. EXPERIMENTAL DETAILS

Polycrystalline samples of $\text{RbAg}_2\text{Cr}[\text{VO}_4]_2$ were synthesized by solid-state reactions as described in Ref. [17]. The sample quality was characterized by Rietveld refinements of x-ray diffraction data [Stoe STADIP diffractometer, Mo $K\alpha_1$, $T = 295$ K, space group $P\bar{3}$, $Z = 1$, $a = 5.4557(2)$ Å, $c = 7.3791(3)$ Å]. Zero-field (ZF) and longitudinal-field (LF) μSR experiments were performed on the GPS beamline at the Paul Scherrer Institute (PSI; Villigen, Switzerland) and on the M20 beamline (TRIUMF Vancouver, Canada) in the temperature range of $T = 2$ –300 K. For μSR measurements below 2 K, the M15 beamline at TRIUMF equipped with a dilution refrigerator was used. The samples were packed in silver foil and attached to the sample holder.

The recorded μSR spectra deliver information about the evolution of the muon spin polarization $P_z(t)$, defined as

$$P_z(t) = \frac{N_B(t) - \alpha N_F(t)}{N_B(t) + \alpha N_F(t)}, \quad (1)$$

where $N_F(t)$ and $N_B(t)$ are the number of positrons counted at the forward and backward detectors, respectively. α is the detector efficiency determined by the forward and backward detectors. The value of α was determined from μSR spectra

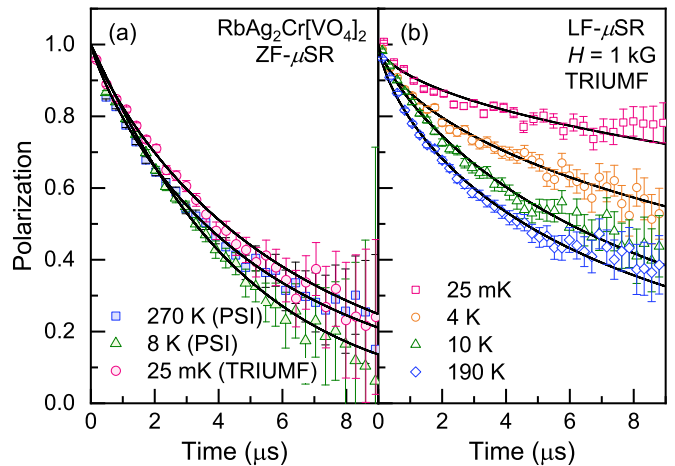


FIG. 2. (a) ZF- and (b) LF- μSR spectra of $\text{RbAg}_2\text{Cr}[\text{VO}_4]_2$ at selected temperatures. LF- μSR measurements were performed in a longitudinal field of $H = 1$ kG to decouple the static contribution. The black solid lines represent fits to the data as described in the text.

in applied weak transverse magnetic field ($H \sim 50$ G) at high temperatures in the paramagnetic state of the compound. We analyzed all of the obtained μSR data with the software package MUSRFIT, the free platform-independent framework for μSR data analysis [18].

The total asymmetry values for the PSI and TRIUMF data are 0.252(2) and 0.237(3), respectively. The time-independent background signal amounts to 2% and 3.7% of the total asymmetry for the experiments at the PSI and TRIUMF and are subtracted from the raw data.

III. RESULTS AND DISCUSSION

To elucidate the nature of the spin dynamics and ground state of $\text{RbAg}_2\text{Cr}[\text{VO}_4]_2$, we performed both ZF- and LF- μSR experiments as a function of temperature and external field. Figure 2 displays representative ZF- and LF- μSR spectra of $\text{RbAg}_2\text{Cr}[\text{VO}_4]_2$ at selected temperatures. In Fig. 2(a), the ZF- μSR spectra reveal a dynamically relaxing muon spin depolarization $P_z(t)$, which shows a small change over a wide temperature range from 270 K to 25 mK. We observe no muon precession or missing initial polarization down to 25 mK, defying the occurrence of long-range magnetic ordering. This observation is fully consistent with the neutron diffraction data and thermodynamic results [17].

Given the small value of the Curie-Weiss temperature and exchange coupling constant ($\Theta_{\text{CW}} \approx -10$ K and $J \approx 0.5$ K obtained from *ab initio* calculations), the ZF muon spin depolarization at elevated temperatures must be dominated by other contributions. Further below we discuss two scenarios. One is based on fluctuations arising from the degeneracy of the symmetry-equivalent t_{2g} orbitals as a source of decoherence. The other involves local vibrations or phonons on the $[\text{VO}_4]^{3-}$ entities in relation to local magnetoelastic effects arising from the slight differences in exchange pathways.

To differentiate the Cr spin from the nuclear contribution to the muon spin depolarization, we carried out LF- μSR experiments under an applied LF of $H = 1$ kG. The applied

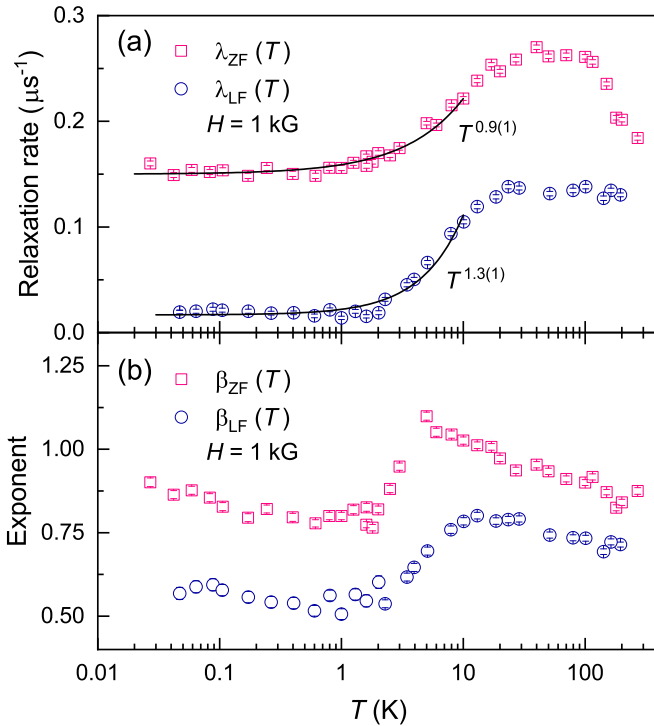


FIG. 3. (a) Temperature dependence of the muon spin relaxation rate λ extracted from ZF- (squares) and LF- μ SR (circles) spectra. (b) Temperature dependence of the exponent β for ZF- (squares) and LF- μ SR (circles) data.

LF decouples the muon spins from the static nuclear fields inherent in the material. Contrary to the ZF- μ SR results above, the LF- μ SR spectra [Fig. 2(b)] show the systematic recovery of the muon spin polarization in the long times as the temperature is lowered. This opposes the notion that the muon spin relaxation is governed by the development of spin-spin correlations upon cooling below the Curie-Weiss temperature. In general, the muon spin depolarization becomes faster with decreasing temperature due to the buildup of the magnetic correlations below Θ_{CW} .

For a quantitative analysis, all of the ZF- and LF- μ SR spectra are fitted with the stretched exponential function $P_z(t) = P_z(0)\exp[-(\lambda t)^\beta]$. Here, λ is the muon spin relaxation rate, and β is the stretching exponent. $P_z(0)$ denotes the initial polarization.

In Fig. 3, we summarize the temperature dependence of the extracted fit parameters for the ZF- and LF- μ SR results. As the temperature is lowered from room temperature, $\lambda_{ZF}(T)$ slightly increases and then flattens out around $T = 100$ K. Upon further cooling below 20 K, $\lambda_{ZF}(T)$ decreases gradually and levels off below 2 K. The application of longitudinal fields suppresses the broad maximum at $T \approx 100$ K and reduces the value of the muon spin relaxation rate. The overall temperature dependence of $\lambda_{LF}(T)$ is quite similar to that of $\lambda_{ZF}(T)$.

This suggests that the muon spin depolarization is governed by an additional mechanism associated with the spin-spin correlations between the Cr moments since the applied LF suppresses other contributions to the muon spin relaxation, such as nuclear dipolar fields and muon spin diffusion. In

order to support the conjecture of an additional mechanism in the high- T paramagnetic state, we estimate the local magnetic field H_{loc} . In the paramagnetic limit, λ is given by $\lambda = 2\gamma_\mu^2 H_{loc}^2 / \nu$, and the exchange fluctuation rate is given by $\nu = \sqrt{z}JS/\hbar$. Here, γ_μ is the muon gyromagnetic ratio, and z is the nearest-neighbor coordination number of the magnetic ion on the triangular lattice. Since the LF- μ SR spectra exhibit a nearly full polarization above 1 kG, we obtain $H_{loc} \sim 100$ G. From this, we calculate the exchange fluctuation rate, $\nu \approx 2.41 \times 10^{11} \text{ s}^{-1}$ and the paramagnetic relaxation rate, $\lambda \sim 0.0006 \mu\text{s}^{-1}$. Since the value of the observed relaxation rate ($0.26 \mu\text{s}^{-1}$ at $T = 100$ K) exceeds the calculated one, the assumption of an additional relaxation mechanism is reasonable.

The origin of additional high- T contributions is far from being clear for $\text{RbAg}_2\text{Cr}[\text{VO}_4]_2$. One thinkable scenario is related to the symmetry-equivalent orbitals carrying the magnetic moment [see plaquette representation in Figs. 1(b) and 1(c)]. At elevated temperatures fluctuations of the occupation number of individual t_{2g} Cr^{3+} orbitals might lead to nonzero local orbital moments seen by the implanted muons. On further cooling below Θ_{CW} , the development of the antiferromagnetic correlations suppresses such orbital fluctuations, giving rise to the threefold-degenerate and energetically minimized orbital configurations discussed above [see Fig. 1(c)]. On the other hand, we recall that the residual magnetic spin entropy at this temperature is still rather large with $\approx 80\%$ [17]. The local fields detected by the muons are averaged out, yielding the effectively reduced orbital contributions. The decrease in the muon spin relaxation rates in Fig. 3(a) for temperatures below Θ_{CW} would therefore reflect the gradual slowing down of orbital fluctuations.

A second proposal is related to lattice degrees of freedom, more specifically to the thermal occupation of vibrational modes of $[\text{VO}_4]^{3-}$ entities at elevated temperatures. Since the exchange interaction between the Cr spins is mediated by this nonmagnetic complex involving several orbitals, vibrational fluctuations of the latter can contribute to the muon spin relaxation. It is interesting to note that there exist both vibrations that differentiate energetically degenerate exchange paths and vibrations that preserve degeneracies, e.g., rotational modes of the $[\text{VO}_4]^{3-}$. In this scenario, the suppression of the broad maximum by a LF of $H = 1$ kG is interpreted as a constraint of the vibrational modes by the applied LF, leading to weakened muon spin diffusion.

At this point we compare our data with other spin systems. In particular, several frustrated magnets show a muon spin relaxation rate that increases and flattens out with lowering temperature [11,19,20], clearly different from $\text{RbAg}_2\text{Cr}[\text{VO}_4]_2$. Compounds with $4f$ ions on frustrated lattices which have been designated as spin-ice and spin-glass materials show nonmonotonic spin relaxations. In the spin-ice material $\text{Dy}_2\text{Ti}_2\text{O}_7$ a broad maximum in the muon spin relaxation rate is observed at 50 K [21]. This has been attributed to a combination of crystal electric field and a slowing down of the Dy^{3+} fluctuation rate. In the unconventional spin-glass material $\text{Y}_2\text{Mo}_2\text{O}_7$ the muon spin relaxation rate shows a power-law decrease $\lambda \propto T^{2.1}$ below the spin-freezing temperature $T_f = 22$ K [22]. A similar power-law like dependence is also observed in $\text{RbAg}_2\text{Cr}[\text{VO}_4]_2$ for temperatures below

Θ_{CW} , with $\lambda_{\text{ZF}}(T)$ and $\lambda_{\text{LF}}(T)$ following a power-law T^n with exponents of $n = 0.9(1)$ and $1.3(1)$, respectively. Such a weak power-law dependence implies that the density of states of low-energy magnetic excitations has only a small energy dependence. This is due to the dominant relation of the temperature and energy dependence of magnetic excitations in the muon spin relaxation. In addition, the small residual relaxation rate of the LF data ($\sim 0.02 \mu\text{s}^{-1}$) below 1 K indicates the nonzero density of states for magnetic excitations in the vicinity of zero energy. Here, however, also the resolution limit of the μSR techniques at such small LF relaxation rates should be mentioned.

The leveling off of $\lambda(T)$ indicates the entrance into a regime of persistent spin dynamics. Such behavior is widely observed for a range of QSL candidates [11,19,20] but is also reported for other ground states, such as spin freezing, spin glass, and weak magnetic order. Therefore, the persistent spin dynamics should not be regarded as a defining signature of a spin liquid. Rather, it is largely due to unconventional low-energy excitations whose origin is still controversial [20,22]. In this sense the observed temperature-dependent behavior of the muon spin relaxation rate supports the presence of unconventional low- T spin excitations pertaining to the $S = 3/2$ TL.

Next, we turn to the stretching exponent obtained from the ZF- and LF- μSR results. The stretching exponent $\beta_{\text{ZF}}(T)$ of the ZF- μSR data initially increases slightly, drops around 5 K, and finally levels off below 2 K. The steplike decrease in $\beta_{\text{ZF}}(T)$ suggests the alteration of the predominant relaxation mechanism as $T \rightarrow 0$ K. The higher-temperature relaxation may be dominated by vibrational modes of the $[\text{VO}_4]^{3-}$ units or fluctuations associated with the t_{2g} -orbital set, while the lower-temperature relaxation is mainly due to the magnetic correlations. The value of $\beta_{\text{ZF}}(T)$ at low temperatures remains close to 1, ruling out the possibility of diluted magnetism [23–25] in $\text{RbAg}_2\text{Cr}[\text{VO}_4]_2$. However, the slightly lower value of $\beta_{\text{ZF}}(T) \sim 0.75\text{--}0.9$ below 2 K implies the presence of residual contributions to the relaxation rate. The application of a longitudinal field leads to the systematic decrease of the stretching exponent. The onset temperature at which the exponent begins to decrease ($T \approx 5$ K) is compatible with the Curie-Weiss temperature. This suggests that the drop in the stretching exponents may reflect the development of short-range magnetic correlations. Remarkably, the reduced value of the exponent by the applied LF contrasts with a typical LF dependence of the exponent reported for spin liquid candidates, in which β tends to increase with increasing field due to the quenched inhomogeneous local fields by an external field. The distinct field dependence of β for $\text{RbAg}_2\text{Cr}[\text{VO}_4]_2$ is due to the very small energy scale of the magnetic exchange interaction ($J \sim 0.5$ K). Thus, even a tiny magnetic field can bring about substantial modulations of the magnetism, as seen by the field-induced gap in the specific heat [17]. In this light, the additional gapped excitation may be responsible for the decrease of β with LF.

Figure 4 presents the LF dependence of the μSR spectra and the relaxation rate $\lambda_{\text{LF}}(H)$, measured at $T = 25$ mK. The LF- μSR spectra at various external fields are well described by the stretched exponential function $P_z(t)$ given above. With increasing longitudinal fields, the muon spin polarization

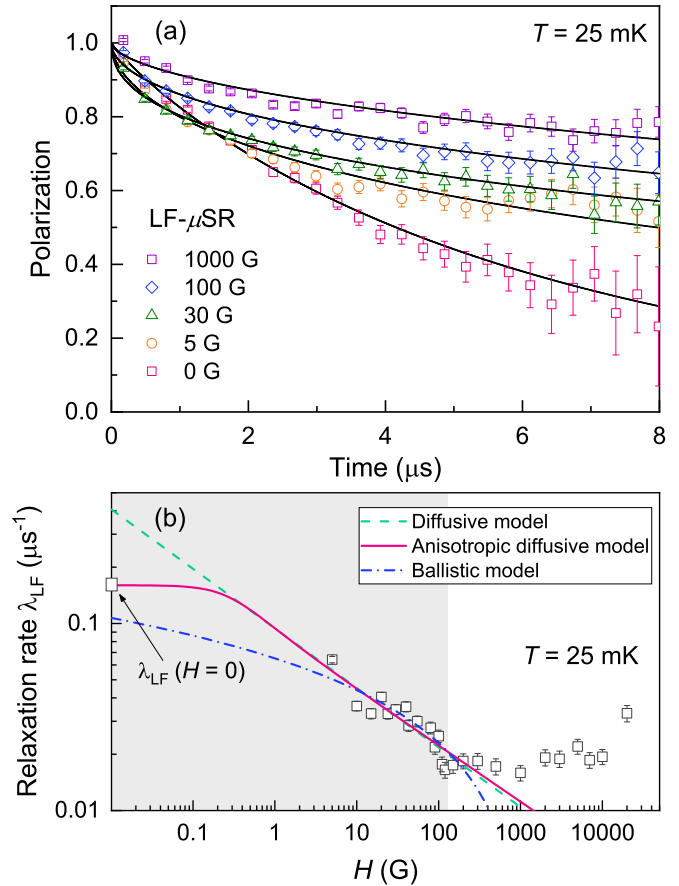


FIG. 4. (a) LF- μSR spectra of $\text{RbAg}_2\text{Cr}[\text{VO}_4]_2$ measured at $T = 25$ mK in an applied longitudinal field of $H = 0\text{--}1000$ G. The solid lines denote fits to the data as described in the text. (b) LF dependence of the muon spin relaxation rate $\lambda_{\text{LF}}(H)$ plotted in a log-log scale. The dashed green, solid red, and blue dot-dashed lines denote fits to 1D spin diffusion, anisotropic spin diffusion, and ballistic spin transport models, respectively. The shaded region represents two distinct muon spin relaxation regimes above and below $H = 120$ G.

tends to recover and almost levels out above 1000 G. The LF dependence of $\lambda_{\text{LF}}(H)$ provides information about the nature of spin excitations since the spin correlation functions are determined by their transport behavior. Three different models are employed to analyze $\lambda_{\text{LF}}(H)$. First, a ballistic spin transport of a two-dimensional system that is characterized by a logarithmic relation $\lambda_{\text{LF}}(H) \propto \ln(J/H)$ is used. Such a model describes the two-dimensional (2D) spinon diffusion within a QSL state [dot-dashed line in Fig. 4(b)] [26]. We obtain an exchange coupling constant $J = 0.124$ T (~ 0.08 K) in the field range of $0 < H \leq 120$ G. This value is one order of magnitude smaller than $J \approx 0.5$ K, inferred from the *ab initio* calculations [17]. Thus, such a ballistic model is not applicable for $\text{RbAg}_2\text{Cr}[\text{VO}_4]_2$.

Second, we use a diffusive model with the dependence $\lambda_{\text{LF}} \propto H^{-n}$, yielding the exponent $n = 0.32(4)$ for $0 < H \leq 120$ G. The obtained exponent is somewhat smaller than the theoretically predicted value of $n = 0.5$ for the one-dimensional diffusive model [26]. Finally, we use the cutoff of a power-law behavior at small external magnetic fields arising

from three-dimensional diffusion, coupling, anisotropy, or, possibly, randomness. Then, $\lambda_{\text{LF}}(H)$ can be expressed [27] as

$$\lambda_{\text{LF}}(H) = \lambda_{\text{LF}}(0) \left(\frac{1 + \sqrt{1 + (H/2H_c)^2}}{2[1 + (H/2H_c)^2]} \right)^n, \quad (2)$$

where $\lambda_{\text{LF}}(0) = 1/\sqrt{2D_{\parallel}D_{\perp}}$ is the constant value for $H < H_c$, with H_c taken as the cutoff magnetic field. For one-dimensional spin chain systems, D_{\parallel} and D_{\perp} represent the fast intrachain and slow interchain diffusion rates. Such a power-law approach can be extended to a two-dimensional QSL. In such cases, the power-law exponent n conveys information on the spin-spin correlations (see below for further discussion). From Eq. (2), we obtain the fit parameters $\lambda_{\text{LF}}(0) = 0.160(5) \mu\text{s}^{-1}$, $H_c = 0.14(7) \text{ G}$, and $n = 0.30(3)$. In order to examine the relevance of ^{51}V nuclear contributions at low fields, we compare ^{51}V NMR data of $\text{BaAg}_2\text{Cu}[\text{VO}_4]_2$ [28] with ac susceptibility data of $\text{RbAg}_2\text{Cr}[\text{VO}_4]_2$. The reported hyperfine coupling constants are ≈ -33 and $-25 \text{ kOe}/\mu_B$ for the two V sites [28], respectively. Taking the low- T value of the ac magnetic susceptibility for $\text{RbAg}_2\text{Cr}[\text{VO}_4]_2$ (0.25 emu/mol at $T = 30 \text{ mK}$ in zero field), we find that the nuclear dipolar field corresponds to $\approx 1.3 \text{ Oe}$ in this case. Such a small value indicates a negligible nuclear dipole contribution from the vanadate to the ZF relaxation in $\text{RbAg}_2\text{Cr}[\text{VO}_4]_2$ even at low temperatures.

The three employed models show very distinct field dependencies below 3 G, as seen in Fig. 4(b). Considering their functional form and the value of $\lambda_{\text{LF}}(0)$, the anisotropic diffusive model provides a reasonable result because the ballistic and diffusive models diverge infinitely as $H \rightarrow 0$. Any anisotropy of the magnetic exchange in $\text{RbAg}_2\text{Cr}[\text{VO}_4]_2$ may contribute to the anisotropic spin diffusion. In passing, we note that a crossover of $\lambda_{\text{LF}}(H)$ to the nearly H independent behavior above 120 G may be related to a field-induced change in spin excitations.

As mentioned above, $\lambda_{\text{LF}}(H)$ exhibits a sublinear power-law behavior with the exponent $n \sim 0.3$ for $H < 120 \text{ G}$. Based on this observation, we will further discuss applicable spin-spin correlation functions at low temperatures. For the exponential spin-spin correlation function $\mathcal{S}(t) = \langle \mathbf{S}(t) \cdot \mathbf{S}(0) \rangle \propto e^{-\nu t}$, the spin excitation spectrum has a Lorentzian spectral density $\mathcal{S}(\omega)$, featuring a quadratic field dependence of $1/\lambda_{\text{LF}} \propto \mathcal{S}(\omega)^{-1} \propto (\gamma_{\mu} H)^2$ [29–31]. The experimentally observed power-law exponent n is significantly smaller than 2, suggesting a nonexponentially decaying spin correlation function.

Rather, the spin correlation function has a power-law decay as a function of time. In the case of a power-law correlation function, $\mathcal{S}(t) \propto t^{-(1-n)}$, the spectral density is given by $\mathcal{S}(\omega) \propto \omega^{-n}$. This approach was used initially for the spin-liquid phase of an $S = 1/2$ Heisenberg antiferromagnetic chain system [27] and was later applied to QSLs of kagome- and pyrochlore-type antiferromagnets [32–35]. For $\text{RbAg}_2\text{Cr}[\text{VO}_4]_2$, the extracted exponent $n \sim 0.3$ implies an algebraic decay of the correlation function $\mathcal{S}(t) \propto t^{-0.7}$ and a spectral density $\mathcal{S}(\omega) \propto \omega^{-0.3}$. We recall that such anomalous spin-spin correlations have also been reported for other QSLs [11,27,35]. In particular, the spin correlation function of $\text{RbAg}_2\text{Cr}[\text{VO}_4]_2$ is quite close to that of the triangular U(1)

QSL material YbMgGaO_4 [$\mathcal{S}(t) \propto t^{-0.66(5)}$] [11]. Therefore, it is tempting to conclude that the Cr spins are likewise correlated without signs of LRO down to 25 mK.

Our ZF- and LF- μSR results for $\text{RbAg}_2\text{Cr}[\text{VO}_4]_2$ reveal features that could be described by a weak dynamic ground state with additional relaxation processes. This behavior is similar to other TL Heisenberg antiferromagnets, such as NaCrO_2 ($S = 3/2$) and NiGa_2S_4 ($S = 1$) [36–38]. The latter exhibit a weak but clear transitionlike anomaly at a finite temperature, however, displaying a QSL-like behavior without conventional LRO. The weak magnetic anomaly has been considered the Z_2 vortex-driven topological transition [39,40]. The magnetic ground state is assigned to a “spin-gel” state, in which the spin correlation has a finite length but the ergodicity is topologically broken. Due to the strongly correlated spins, a spontaneous internal magnetic field develops below T_C , as revealed by μSR experiments [36–38]. In contrast to the spin-gel materials, $\text{RbAg}_2\text{Cr}[\text{VO}_4]_2$ manifests the absence of spontaneous internal magnetic fields down to 25 mK ($\Theta_{\text{CW}} = -10 \text{ K}$). The steplike feature in the exponent can be considered a partial spin freezing. However, since β remains close to 1, the temperature dependence of the exponent should be attributed to a crossover of the dominant relaxation mechanism. The similar but apparently different behavior of $\text{RbAg}_2\text{Cr}[\text{VO}_4]_2$ from a spin-gel state suggests that the dynamic magnetism in $\text{RbAg}_2\text{Cr}[\text{VO}_4]_2$ is closer to a QSL than a spin gel.

In the following, we will discuss more general arguments towards the suppression of LRO in $\text{RbAg}_2\text{Cr}[\text{VO}_4]_2$ as well as its relation to the distortion of the threefold symmetry ($P\bar{3}$ to $C2/c$) introduced by smaller A site cations. Previous theoretical studies considered different scenarios that destabilize magnetic order of the TL based on fundamental approaches [1,12–16]. The arguments were found to be rather independent of the spin magnitude. Spin fluctuations may be enhanced, and LRO may be suppressed by a proximity to a Mott transition, i.e., a small charge gap, and by alterations of the spin exchange Hamiltonian, namely, single-ion anisotropies and longer-range exchange (ring exchange). As there is no evidence for metallicity and the given compound has a yellow-brownish color, we consider only spin degrees of freedom. Single-ion anisotropies for $S > 1/2$ are related to spin-orbit (SO) interactions. From thermodynamic and spectroscopic investigations it is known that Cr^{3+} has a rather small SO coupling [41]. On the other hand, single-ion anisotropies with strength relevant to suppress LRO should lead to Berezinskii-Kosterlitz-Thouless (BKT) transitions [42] with $T_{\text{BKT}} \sim 0.1J^3S/D^2 \sim 1.62 \text{ K}$, with the SO coupling constant D [43]. As there is no experimental evidence for such instabilities, we do not further consider anisotropies here.

The role of longer-range exchange processes in the suppression of LRO is well known but is difficult to quantify as it overlaps or is superimposed on conventional superexchange processes. Arguments in favor of such higher-order processes could be based on the exchange paths via $[\text{VO}_4]^{3-}$ entities [see Fig. 1(b)]. These groups contain unoccupied d electron states known to amplify higher-order processes. In a previous study these arguments were considered a side line and based on band structure calculations. No strong evidence for longer-range exchange has been found [17].

Within this chain of arguments the remarkable dependence of the ordering temperature on the size of the A cation, the orientation of the $[\text{VO}_4]^{3-}$ entities, and the global distortion of the TL should be highlighted again. In Fig. 1(c) it is shown that the three occupied t_{2g} orbitals represented by the three plaquettes of the CrO_6 octahedra cover the undistorted TL in a threefold manner. With $A = \text{Ag}^+$ this degeneracy is lifted, and LRO is induced [Fig. 1(a)]. Therefore, we conclude that the combination of the complex exchange path via $[\text{VO}_4]^{3-}$ entities and the large degeneracy of the symmetry-equivalent t_{2g} orbitals is the essential key to the suppression of LRO. Although a microscopic description of this mechanism in TL materials remains elusive, future theoretical and experimental studies could further elaborate on this interplay.

IV. CONCLUSION

The $S = 3/2$ TL compound $\text{RbAg}_2\text{Cr}[\text{VO}_4]_2$ was investigated by ZF- and LF- μ SR. We corroborated the absence of static magnetism down to 25 mK. Additionally, our results revealed both the development of anomalous spin dynamics and alterations of the predominant relaxation mechanism with decreasing temperature. The field dependence of the LF muon

relaxation rate $\lambda_{\text{LF}}(H)$ shows a power-law behavior, implying the presence of algebraic spin-spin correlations. Therefore, our findings suggest a way to suppress LRO in 2D TL antiferromagnets. The temperature-independent muon spin relaxation rates $\lambda_{\text{ZF}}(T)$ and $\lambda_{\text{LF}}(T)$ below $T \leq 2$ K indicate the existence of unconventional spin excitations, providing additional supportive evidence for a dynamic ground state. The discovery of such exotic spin excitations on the TL with a large spin ($S = 3/2$) deserves further investigation to examine the exact magnetic ground state and the underlying mechanism therein.

ACKNOWLEDGMENTS

We would like to thank B. Hitti (TRIUMF, Vancouver, Canada) for technical support. This work was supported by Korea Research Foundation (KRF) Grants No. 2017R1A2B3012642, No. 2019-0571, and No. 2013M7A1A1075764 funded by the Korea government (MEST). A.M. acknowledges the Carl-Zeiss-Foundation. Support by the German Science Foundation (DFG), DFG INST 247/875-1, DFG Le967/16-1, and DFG EXC 2123, is gratefully acknowledged.

-
- [1] G. H. Wannier, *Phys. Rev.* **79**, 357 (1950).
 [2] L. Balents, *Nature (London)* **464**, 199 (2010).
 [3] B. Bernu, C. Lhuillier, and L. Pierre, *Phys. Rev. Lett.* **69**, 2590 (1992).
 [4] H. Kawamura, *J. Phys.: Condens. Matter.* **10**, 4707 (1998).
 [5] L. Capriotti, A. E. Trumper, and S. Sorella, *Phys. Rev. Lett.* **82**, 3899 (1999).
 [6] L. Savary and L. Balents, *Rep. Prog. Phys.* **80**, 016502 (2017).
 [7] N. E. Amuneke, J. Tapp, C. R. de la Cruz, and A. Möller, *Chem. Mater.* **26**, 5930 (2014).
 [8] J. S. White, C. Niedermayer, G. Gasparovic, C. Broholm, J. M. S. Park, A. Y. Shapiro, L. A. Demianets, and M. Kenzelmann, *Phys. Rev. B* **88**, 060409(R) (2013).
 [9] S. Yamashita, Y. Nakazawa, M. Oguni, Y. Oshima, H. Nojiri, Y. Shimizu, K. Miyagawa, and K. Kanoda, *Nat. Phys.* **4**, 459 (2008).
 [10] S. Yamashita, T. Yamamoto, Y. Nakazawa, M. Tamura, and R. Kato, *Nat. Commun.* **2**, 275 (2011).
 [11] Y. Li, D. Adroja, P. K. Biswas, P. J. Baker, Q. Zhang, J. Liu, A. A. Tsirlin, P. Gegenwart, and Q. Zhang, *Phys. Rev. Lett.* **117**, 097201 (2016).
 [12] T. Shimokawa, K. Watanabe, and H. Kawamura, *Phys. Rev. B* **92**, 134407 (2015).
 [13] E. Ghorbani, L. F. Tocchio, and F. Becca, *Phys. Rev. B* **93**, 085111 (2016).
 [14] G. Misguich, C. Lhuillier, B. Bernu, and C. Waldtmann, *Phys. Rev. B* **60**, 1064 (1999).
 [15] H.-Y. Yang, A. M. Läuchli, F. Mila, and K. P. Schmidt, *Phys. Rev. Lett.* **105**, 267204 (2010).
 [16] P. A. Maksimov, Z. Zhu, S. R. White, and A. L. Chernyshev, *Phys. Rev. X* **9**, 021017 (2019).
 [17] J. Tapp, C. R. de la Cruz, M. Bratsch, N. E. Amuneke, L. Postulka, B. Wolf, M. Lang, H. O. Jeschke, R. Valentí, P. Lemmens, and A. Möller, *Phys. Rev. B* **96**, 064404 (2017).
 [18] A. Suter and B. M. Wojek, *Phys. Procedia* **30**, 69 (2012).
 [19] P. Mendels, F. Bert, M. A. de Vries, A. Olariu, A. Harrison, F. Duc, J. C. Trombe, J. S. Lord, A. Amato, and C. Baines, *Phys. Rev. Lett.* **98**, 077204 (2007).
 [20] A. Yaouanc, P. Dalmas de Reotier, A. Bertin, C. Marin, E. Lhotel, A. Amato, and C. Baines, *Phys. Rev. B* **91**, 104427 (2015).
 [21] S. R. Dunsiger, A. A. Aczel, C. Arguello, H. Dabkowska, A. Dabkowski, M. H. Du, T. Goko, B. Javanparast, T. Lin, F. L. Ning, H. M. L. Noad, D. J. Singh, T. J. Williams, Y. J. Uemura, M. J. P. Gingras, and G. M. Luke, *Phys. Rev. Lett.* **107**, 207207 (2011).
 [22] S. R. Dunsiger, R. F. Kiefl, K. H. Chow, B. D. Gaulin, M. J. P. Gingras, J. E. Greedan, A. Keren, K. Kojima, G. M. Luke, W. A. MacFarlane, N. P. Raju, J. E. Sonier, Y. J. Uemura, and W. D. Wu, *Phys. Rev. B* **54**, 9019 (1996).
 [23] Y. J. Uemura, T. Yamazaki, D. R. Harshman, M. Senba, and E. J. Ansaldo, *Phys. Rev. B* **31**, 546 (1985).
 [24] I. A. Campbell, A. Amato, F. N. Gygax, D. Herlach, A. Schenck, R. Cywinski, and S. H. Kilcoyne, *Phys. Rev. Lett.* **72**, 1291 (1994).
 [25] A. Keren, P. Mendels, I. A. Campbell, and J. Lord, *Phys. Rev. Lett.* **77**, 1386 (1996).
 [26] F. L. Pratt, S. J. Blundell, P. A. Pattenden, W. Hayes, K. H. Chow, A. P. Monkman, T. Ishiguro, K. Ishida, and K. Nagamine, *Hyperfine Interact.* **106**, 33 (1997).
 [27] F. L. Pratt, S. J. Blundell, T. Lancaster, C. Baines, and S. Takagi, *Phys. Rev. Lett.* **96**, 247203 (2006).
 [28] Y. Krupskaya, M. Schäpers, A. U. B. Wolter, H. Grafe, E. Vavilova, A. Möller, B. Büchner, and V. Kataev, *Z. Phys. Chem.* **231**, 759 (2017).

- [29] R. S. Hayano, Y. J. Uemura, J. Imazato, N. Nishida, T. Yamazaki, and R. Kubo, *Phys. Rev. B* **20**, 850 (1979).
- [30] A. G. Redfield, *IBM J. Res. Dev.* **1**, 19 (1957).
- [31] A. Yaouanc and P. Dalmas de Rotier, *Muon Spin Rotation, Relaxation, and Resonance: Applications to Condensed Matter* (Oxford University Press, Oxford, 2011).
- [32] A. Keren, J. S. Gardner, G. Ehlers, A. Fukaya, E. Segal, and Y. J. Uemura, *Phys. Rev. Lett.* **92**, 107204 (2004).
- [33] E. Kermarrec, P. Mendels, F. Bert, R. H. Colman, A. S. Wills, P. Strobel, P. Bonville, A. Hillier, and A. Amato, *Phys. Rev. B* **84**, 100401(R) (2011).
- [34] E. Kermarrec, A. Zorko, F. Bert, R. H. Colman, B. Koteswararao, F. Bouquet, P. Bonville, A. Hillier, A. Amato, J. van Tol, A. Ozarowski, A. S. Wills, and P. Mendels, *Phys. Rev. B* **90**, 205103 (2014).
- [35] M. Gomilšek, M. Klanjšek, M. Pregelj, H. Luetkens, Y. Li, Q. M. Zhang, and A. Zorko, *Phys. Rev. B* **94**, 024438 (2016).
- [36] A. Yaouanc, P. Dalmas de Réotier, Y. Chapuis, C. Marin, G. Lapertot, A. Cervellino, and A. Amato, *Phys. Rev. B* **77**, 092403 (2008).
- [37] S. Zhao, P. Dalmas de Réotier, A. Yaouanc, D. E. MacLaughlin, J. M. Mackie, O. O. Bernal, Y. Nambu, T. Higo, and S. Nakatsuji, *Phys. Rev. B* **86**, 064435 (2012).
- [38] A. Olariu, P. Mendels, F. Bert, B. G. Ueland, P. Schiffer, R. F. Berger, and R. J. Cava, *Phys. Rev. Lett.* **97**, 167203 (2006).
- [39] H. Kawamura and A. Yamamoto, *J. Phys. Soc. Jpn.* **76**, 073704 (2007).
- [40] H. Kawamura, A. Yamamoto, and T. Okubo, *J. Phys. Soc. Jpn.* **79**, 023701 (2010).
- [41] A. J. Wojtowicz, M. Grinberg, and A. Lempicki, *J. Lumin.* **50**, 231 (1991).
- [42] P.-É. Melchy and M. E. Zhitomirsky, *Phys. Rev. B* **80**, 064411 (2009).
- [43] A. Sen, F. Wang, K. Damle, and R. Moessner, *Phys. Rev. Lett.* **102**, 227001 (2009).